DFT Theoretical Study on the Reaction Mechanism of the Nitrate Radical with Alkenes: 2-Butene, Isobutene, 2-Methyl-2-butene, and 2,3-Dimethyl-2-butene

M. Pilar Pérez-Casany, Ignacio Nebot-Gil,* and José Sánchez-Marín

Department de Química Física, Institute of Molecular Sciences, Universitat de València, C/Dr. Moliner, 50, 46100 Burjassot, València, Spain

Received: February 18, 2000; In Final Form: July 31, 2000

A general mechanism for the reactions of the NO_3 radical with 2-butene, isobutene, 2-methyl-2-butene, and 2,3-dimethyl-2-butene is proposed on the basis of density functional theory (DFT) calculations. This mechanism is compared with previously reported model experimental kinetic studies at low pressures and temperatures in anaerobic conditions. In our theoretical proposal of mechanism, the initial step is the addition of the NO_3 radical to the double bond. For the systems showing different substitution on both sides of the double bond, two adducts have been obtained, one following the Markovnikov rule and the other with the anti-Markovnikov orientation. Starting from the adduct we have found that three main reaction pathways follow. The first one leads to epoxide and NO_2 formation, the second to carbonyl compounds, and the third, through the cleavage of the C−C bond, to carbonyl compounds with a lower number of carbon atoms than the original substrate and NO. The theoretical proposal of mechanism leads to the following products: (a) for 2-butene, 2,3-dimethyloxirane, butanone, and ethanal; (b) for isobutene, 2-methylepoxypropane, 2-methylpropanal, butanone, propanone, and formaldehyde; (c) for 2-methyl-2-butene, 2-methylepoxybutane, 3-methylbutanone, propanone, 2-dimethylpropanal, and ethanal; (d) for 2,3-dimethyl-2-butene, 2,3-dimethylepoxybutane, 3-dimethylbutanone, and propanone. In all cases, NO_2 and NO are also obtained as products. The geometry of all the involved stationary points in the potential energy hypersurface has been optimized at the DFT level with the B3LYP functional and a 6-31G* basis set. All these conformations were characterized at the same calculation level.

1. Introduction

The NO_3 oxidation reactions with unsaturated compounds represent an important sink of these species in the nighttime troposphere.[1] NO_3 is well-known to add to the double bond through an electrophilic mechanism, and the radical adduct formed allows a free rotation around the C−C bond. Kinetic and product analysis has shown that the reactions between the nitrate radical and alkenes are relatively fast with reaction rate coefficients increasing as the alkyl substitution increases.[2]

Experimental kinetic studies on reactions of interest for the atmospheric chemistry are carried out in atmospheric-like realistic conditions as well as at inert gas conditions in order to gain fundamental knowledge on the mechanism and product distribution. Hjorth et al.[3] studied the products of reactions of alkyl substituted ethene with NO_3 in air at 740 Torr and 295 K, where more than one hydrogen atom is substituted. These authors found carbonyl, nitroxycarbonyl, nitroxy alcohol, and dinitrate species as main products, being the product distribution dependent on the alkyl substitution around the double bond. Wille et al.[4,5] obtained the corresponding epoxides as main products at low pressures, although they did not neglect the formation of carbonyl compounds. Skov et al.[6] found that epoxides were the main products at low pressures in argon. However, in air at 740 Torr, epoxides were below the detection limit in the case of *cis*- and *trans*-2-butene, and in the case of 2,3-dimethyl-2-butene, an epoxide yield of 17.4% was measured.

Berndt et al.,[7] in a study on the NO_3 radical and the 2,3-dimethyl-2-butene reaction, found tetramethyloxirane as the main product when inert gas was used. Acetone is also found in a synthetic air condition, but under tropospheric conditions still 20% of tetramethyloxirane was found. The study on the reactions between the nitrate radical and 2-methyl-2-butene, isobutene, *trans*-butene, 1-butene, and propene showed as main products epoxides, nitroxy−carbonyl compounds, and ketones or aldehydes, with the product distribution being a function of the pressure.[8]

To complement model experimental studies, in two previous papers,[9,10] we have studied, by means of quantum chemistry theoretical methods, the addition reaction mechanism of the NO_3 radical to an unsubstituted and a methyl monosubstituted double bond, the ethene and the propene, respectively. In both cases, epoxide, aldehyde, ketone, and NO_2 were found as main products. NO and propenol were also found in the case of the propene. In the ethene mechanism, the oxirane was the product kinetically more favored. On the contrary, in the propene mechanism, an equilibrium distribution was obtained, between epoxide, NO_2, formaldehyde, ethanal, and NO.

In this work, we present a density functional theoretical study on the mechanism of the reaction between the nitrate radical and *cis*- and *trans*-2-butene, isobutene, 2-methyl-2-butene, and 2,3-dimethyl-2-butene. The theoretical study includes only the addition of the NO_3 radical to the double bond and further unimolecular rearrangements. Thus, we have not considered the reaction between the formed intermediates or products with molecular oxygen that will be very important in the actual atmosphere.

One goal of this study is to compare the mechanisms of the different substituted alkenes with the corresponding ones for

* To whom correspondence should be addressed. FAX: +34 96 398 3156. E-mail: Ignacio.Nebot@uv.es.

10.1021/jp000666f CCC: $19.00
Published on Web 10/25/2000

the ethene and propene. The main objectives are (a) to study the effect of the position and number of the substituent groups linked to the double bond on the reaction rate and (b) to establish a relationship between all of the mechanisms studied in order to obtain a generalization, which could be used on larger molecules.

Also, this work pretends to provide information on the whole mechanism in order to gain knowledge on the main reaction products, as well as all of the intermediates. All these could be susceptible to an attack by oxygen or other molecules, such as NO_2, NO_3, or SO_2, giving other pollutant products. In this way, the theoretical studies can complement model experiences.

This study has been performed in two steps. First, a prospective study of the potential energy surface was done with the AM1 method. Then, all the found relevant stationary points were optimized and characterized at the DFT level with the B3LYP density functional. The computational aspects are detailed in section 2. In section 3, the calculated reaction mechanism is presented and discussed in a general way. Section 3.1 describes the reaction pathway leading to the adduct formation. Section 3.2 shows the pathway leading to the epoxide formation. In section 3.3, the pathway leading to carbonyl compounds is described. Section 3.4 shows the pathway leading to carbonyl compounds and NO through C−C bond cleavage. In section 3.5, the reaction energy profiles and the energy barrier heights involved for all the studied reaction pathways are compared. The conclusions are enumerated in section 4.

2. Computational Details

The potential energy hypersurfaces (PES) have been explored at a semiempirical AM1[11] level, and the stationary points have been classified according to their significance for the reactions, in a way similar to that of previous papers.[9,10,12] The AM1 results have not been included in the results section. Taking the AM1 optimized geometries as starting point, all the relevant stationary points have been optimized again within the density functional theory (DFT) framework, by using the B3LYP functional. This functional is based on Becke's three-parametrization adiabatic connection method (ACM) and consists of a combination of Slater,[13] Hartree−Fock,[14] and Becke[15] exchange functionals, the Vosko, Wilk, and Nusair (VWN) local correlation functional,[16] and the Lee, Yang, and Parr[17] nonlocal correlation functional. Given the size of the calculated molecules and the complexity of the involved geometry optimizations, and the number of stationary points involved (minima and transition states), B3LYP has been chosen as a method giving reasonable results for such large systems.[10]

The stationary points optimized at the DFT level have been characterized as minima (the number of imaginary frequencies NIMAG = 0) or transition states (NIMAG = 1) by calculating the Hessian matrix and analyzing the vibration normal modes. The eigenvector-following and transition-state techniques[18] have been used for the geometry optimization of the minima and transition states. The Berny analytical gradient[19] has been used for geometry optimizations of the minima and transition states at the B3LYP level. The 6-31G* Pople split valence[20,21] basis set, including d-type polarization functions on non-hydrogen atoms, has been used in the calculations. Frequencies and zero point corrections were also calculated at the same B3LYP/6-31G* theoretical level, without scaling.

The calculations have been carried out with the GAUSSIAN 94 series of programs[22] on the two IBM RS6000-590H and the IBM SP2 computers of the Theoretical Chemistry Group of the University of Valencia and on the SGI Origin 2000 computer of the University of Valencia Computer Centre.

3. Results and Discussion

The mechanisms for the reactions of the NO_3 radical with 2-butene, 2-methylpropene, 2-methyl-2-butene, and 2,3-dimethyl-2-butene, respectively, have been calculated by means of quantum chemistry theoretical methods. Only those stationary points on the potential energy hypersurface (PES) related with a chemical reaction have been included in the mechanism proposals. Since the four studied reactions are similar, we have summarized them in a whole reaction mechanism, to generalize the addition reaction of the NO_3 radical to all unsaturated $C_2H_{4-n}Me_n$ ($n = 0-4$) organic compounds.

Three main reaction pathways have been found. The first one leads to epoxide formation, the second to the formation of carbonyl compounds, and the third one, through the cleavage of the C−C bond, to carbonyl compounds of a shorter carbon chain. What reaction products are obtained depends on the substitution degree on the double bond. Thus, for the reaction mechanism involving the 2-butene, the proposed products are 2,3-dimethyloxirane, butanone, and ethanal. For the 2-methylpropene mechanism, the main products would be 2-methylepoxypropane, 2-methylpropanal, butanone, propanone, and formaldehyde. When a third methyl group is present on the double bond, as in case of the 2-methylbutene, the main products would be 2-methylepoxybutane, 3-methylbutanone, propanone, 2-dimethylpropanal, and ethanal. If there is a fourth methyl group on the double bond, as in the case of the 2,3-dimethylbutene, the main products are 2,3-dimethylepoxybutane, 3-dimethylbutanone, and propanone. In all the cases NO_2 and NO are also present as products.

3.1. Adduct Formation. The first step in the reaction mechanism is the formation of a radical adduct, MO, in a way similar to the case of the addition mechanism of the nitrate radical to ethene[23] and propene,[10] respectively. The formation of a prereaction van der Waals complex has been used in some studies to explain the negative values found for the experimental activation energies.[24,25] These prereaction complexes are due to long-range interactions between reactant molecules, and they are common in most chemical reactions involving bond breaking. However, they can normally be ignored since they are chemically meaningless. Therefore we can assume that the reactants form a van der Waals complex at long distances, as we have found for the addition reaction theoretical mechanism of NO_3[23] and OH[26] to ethene. van der Waals prereaction complexes have also been reported in other quantum chemical studies on the OH addition reaction to alkenes.[27−29] Then, from this van der Waals complex, a transition state would lead to a radical adduct. We can also assume that the energy of this transition state will be very close to that of the van der Waals complex, due to the long intermolecular distances involved. In some cases, the transition-state energy could be lower than the reactants energy, showing negative activation energies,[1] as it is found for the OH + ethene case in both experimental[30−34] and theoretical studies.[27−29,35−37]

We have found transition states that lead to the different radical adducts. The relative to reactants energies of the transition states leading to the Markovnikov oriented addition (on the more substituted carbon atom), TSM, are −4.40 (for the 2-butene, R1), −4.64 (isobutene, R2). No significant differences were found for *cis*- and *trans*-2-butene. However, we were not able to completely optimize the TSM geometry for the 2-methyl-2-butene and the 2,3-dimethyl-2-butene cases,

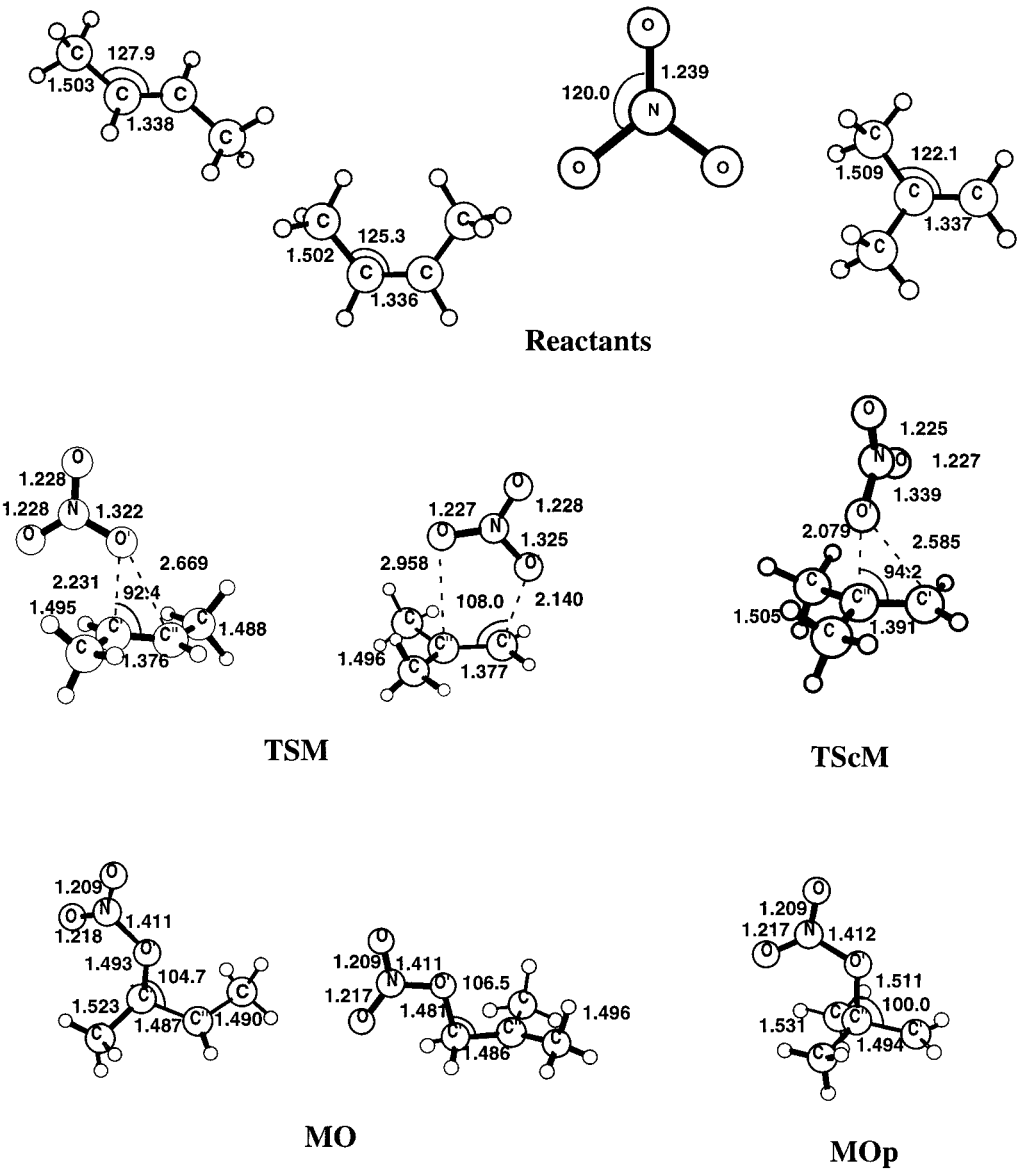

Figure 1. Addition reaction mechanism of the NO_3 radical to 2-butene and isobutene: B3LYP/6-31G* optimized geometry of the PES stationary points in the adduct formation pathway. White atoms correspond to nonrelevant hydrogen atoms.

so an estimation was made by fixing the O'−C' distance and optimizing the rest of the parameters (Figure 1S). This is a frequent problem with DFT calculations on long-range transition states in addition reactions. The energies of these approximated TSMs are −7.40 (2-methyl-2-butene, R3) and −7.47 kcal/mol (2,3-dimethyl-2-butene, R4). Energy values will be discussed in section 3.5. The transition vector is linked to the C'−O' stretching. The imaginary frequencies associated with the TSM are 135*i* (R1) and 119*i* (R2) cm^{-1}. In the case of the two approximated TSMs, two imaginary frequencies are found for each, the first one corresponding to the C'−O' stretching and the second one to the relative orientation of the two fragments. The values are 128*i* and 41*i* (R3) cm^{-1} and 72*i* and 48*i* (R4) cm^{-1}. All the frequency values are very small as corresponds to transition states close to weak van der Waals complexes on flat potential energy surfaces. The presence of a second imaginary frequency in the approximate transition states means that the energy of these conformations represents only an upper bound to the energy of the true transition state.

An anti-Markovnikov oriented addition reaction pathway has also been found for R2 and R3, where the two carbons on the double bond are asymmetrically substituted. Thus, in the case of the isobutene, the involved transition state, TScM, has a relative to the reactants energy of −2.80 kcal/mol and the transition vector is linked to the C''−O' stretching with an associated imaginary frequency of 227*i* cm^{-1}. In the case of the 2-methyl-2-butene, we were not able to completely optimize the TScM conformation and then an estimation was done by fixing the O'−C'' distance. The relative energy of this estimated TScM is −4.39 kcal/mol and shows two imaginary frequencies, one corresponding to a transition vector linked to the C''−O'stretching of 82*i* cm^{-1} and the other to that of 52*i* cm^{-1} associated with the relative orientation of the two fragments.

Thus, a scheme of this first reaction step would be The

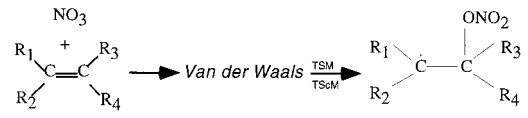

B3LYP/6-31G* optimized geometries for the PES stationary points involved in this step are shown in Figures 1 and 1S.

3.2. Epoxide Formation. We have found that three reaction pathways originate from MO, leading to different products. The

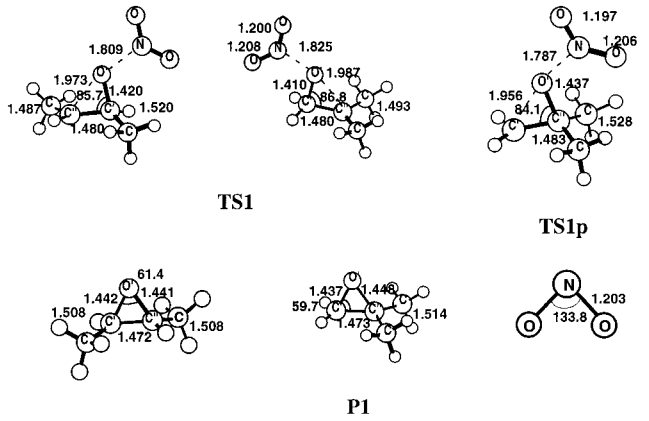

Figure 2. Addition reaction mechanism of the NO_3 radical to 2-butene and isobutene: B3LYP/6-31G* optimized geometry of the PES stationary points in the epoxide formation pathway. White atoms correspond to nonrelevant hydrogen atoms.

first pathway leads from the adduct, MO, to the formation of the corresponding epoxide, P1, and NO_2 in an exothermic way by 21.05 (R1), 18.92 (R2), 20.86 (R3), and 25.43 (R4) kcal/mol (all the energy values are done relative to the corresponding reactants). This step is similar to that found in the previous studies on the reaction mechanisms of the NO_3 radical and the ethene[9] and propene,[10] respectively. The transition states connecting the MO and P1 minima, TS1, are at −3.26 (R1), −4.06 (R2), −5.85 (R3), and −5.97 (R4) kcal/mol. In all the four mechanisms, the reaction coordinate involves the closure of the O'−C'−C'' angle and the enlargement of the O'−N distance (Figures 2 and 2S), and the associated imaginary frequencies are 658*i* (R1), 626*i* (R2), 620*i* (R3), and 581*i* (R4) cm^{-1}. The scheme of this reaction pathway is then

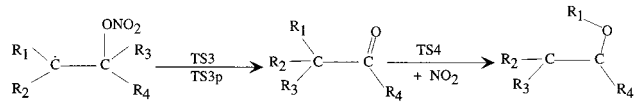

Figures 2 and 2S show the B3LYP/6-31G* optimized geometries of the PES stationary points involved in this step. It should be pointed out that the optimized geometries of the four TS1 are very similar, the largest difference being 0.03 Å in distances and 1° in angles. When going from the 2-butene to the tetramethylethylene the C'−C'' distance increases from 1.480 to 1.501 Å, due to the methyl groups hindrance effect.

In the cases of isobutene and 2-methyl-2-butene, a reaction pathway leads also to the epoxide, P1, but starting from the anti-Markovnikov radical adduct, MOp, in an exothermic way by 25.70 (R2) and 25.70 (R3) kcal/mol. The involved transition states, TS1p, are at 0.20 (R2) and −2.91 (R3) kcal/mol and show imaginary frequencies of 669*i* (R2) and 626*i* (R3) cm^{-1}.

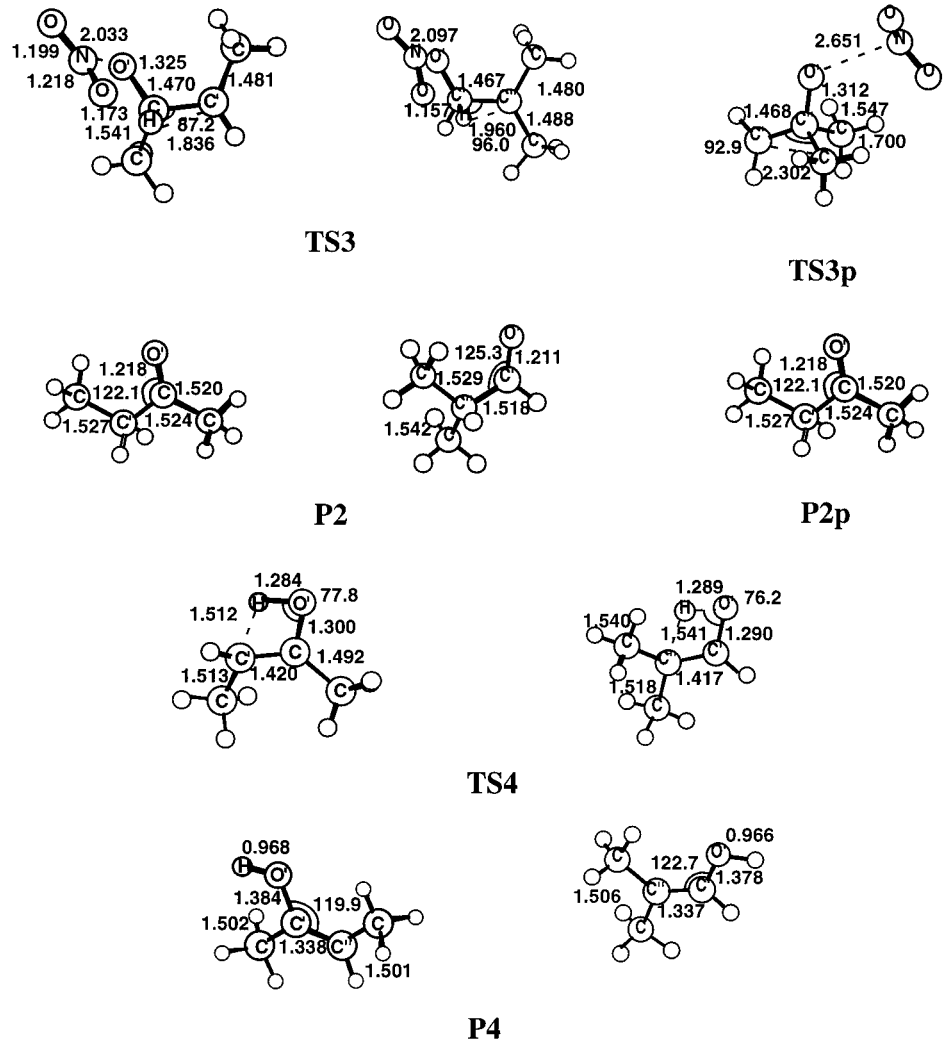

Figure 3. Addition reaction mechanism of the NO_3 radical to 2-butene and isobutene: B3LYP/6-31G* optimized geometry of the PES stationary points in the carbonyl formation pathway. White atoms correspond to nonrelevant hydrogen atoms.

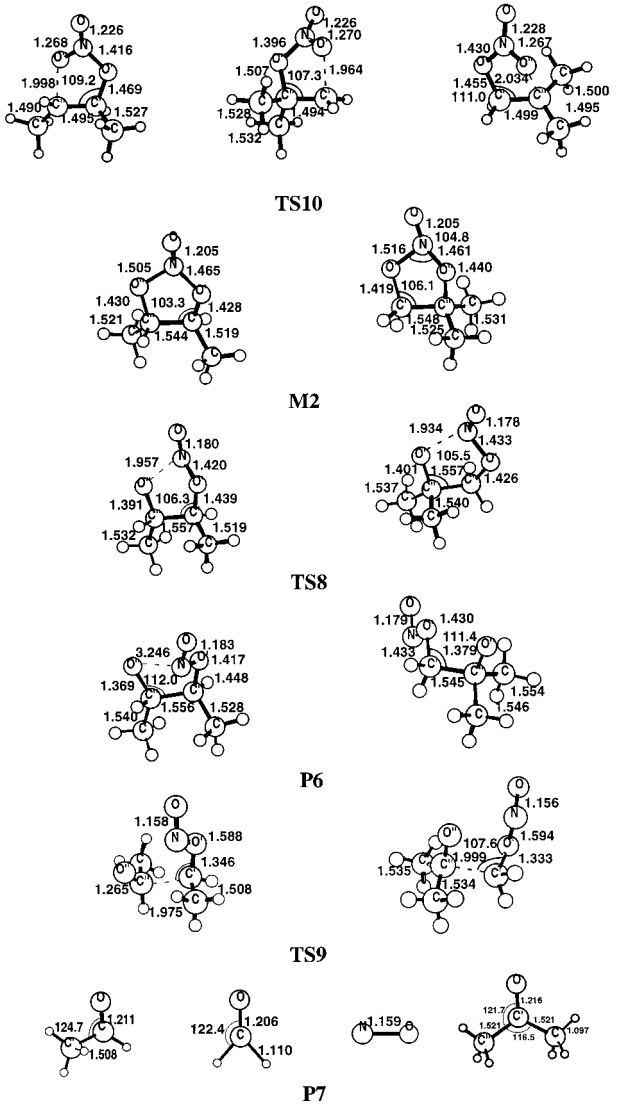

Figure 4. Addition reaction mechanism of the NO_3 radical to 2-butene and isobutene: B3LYP/6-31G* optimized geometry of the PES stationary points in the C−C cleavage pathway. White atoms correspond to nonrelevant hydrogen atoms.

As in the TS1 case, the geometries are very similar and the C'−C'' distance is 1.483 and 1.491 Å for R2 and R3, respectively (Figures 2 and 2S).

3.3. Carbonyl Formation. The second pathway in the global reaction mechanism leads from the initial adducts to the successive formation of NO_2 and carbonyl compounds, P2, and then, from them, to their enol forms, P4. This reaction pathway is not possible for the 2,3-dimethyl-2-butene, due to the huge hindrance effect of the methyl groups for the 1,2-methyl shift step:

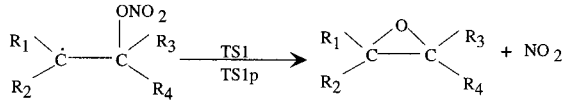

The first step in this reaction pathway is produced in an exothermic way by 46.56 (R1), 37.92 (R2), and 42.65 (R3) kcal/mol. The involved transition states, TS3, are at 9.64 (R1), 6.10 (R2), and 6.68 (R3) kcal/mol and show imaginary frequencies of 532*i* (R1), 303*i* (R2), and 294*i* (R3) cm^{-1}. The associated transition vector going from MO to P2 involves a 1,2-hydrogen shift and the enlargement of the O'−N distance (see Figure 3),

TABLE 1: 2-Butene and NO_3 Radical Reaction. B3LYP/6-31G(d) Total Energies (au), Experimental Enthalpies of Formation, and B3LYP/6-31G(d) and Experimental[38] Energies Relative to the Reactants (kcal/mol) for All PES Stationary Points Relevant to the Theoretical Proposal of the Reaction Mechanism[a]

stationary points	E(B3LYP)	ΔH_f°	ΔE(B3LYP)	ΔH_r°
NO_3 + *trans*-2-butene	−437.335 193	14.90	0.00	0.00
Cis-2-butene	−437.332 910	15.93	1.43	1.03
TSM	−437.454 654		−4.40	
MO	−437.474 662		−15.77	
TS1	−437.452 451		−3.26	
P1	−437.507 367		−36.82	
P2	−437.542 762	−49.16	−60.43	−64.06
TS3	−437.428 073		9.64	
TS4	−437.429 262		6.86	
P4	−437.515 142		−43.24	
TS10	−437.450 226		−0.61	
M2	−437.498 810		−29.26	
TS8	−437.492 541		−26.54	
P6	−437.494 592		−28.67	
TS9	−437.485 052		−24.60	
P7	−437.548 394	−57.68	−61.41	−72.58

[a] Zero point correction has been included in the B3LYP energy differences.

TABLE 2: Isobutene and NO_3 Radical Reaction. B3LYP/6-31G(d) Total Energies (au), Experimental Enthalpies of Formation, and B3LYP/6-31G(d) and Experimental[38] Energies Relative to the Reactants (kcal/mol) for All PES Stationary Points Relevant to the Theoretical Proposal of the Reaction Mechanism[a]

stationary points	E(B3LYP)	ΔH_f°	ΔE(B3LYP)	ΔH_r°
NO_3 + isobutene	−437.444 086	13.59	0.00	0.00
TSM	−437.455 505		−4.64	
TScM	−437.452 416		−2.80	
MO	−437.477 125		−16.83	
TS1	−437.453 965		−4.06	
P1	−437.505 879		−35.75	
TS3	−437.433 771		6.10	
P2	−437.531 535	−43.68	−53.01	−57.27
TS4	−437.411 600		18.54	
P4	−437.511 424		−40.58	
MOp	−437.464 876		−10.05	
TS1p	−437.446 868		0.20	
TS3p	−437.407 371		22.69	
P2p	−437.542 762	−49.16	−60.18	−62.75
TS10	−437.452 775		−2.09	
TS11	−437.446 077		1.99	
M2	−437.496 559		−27.83	
TS8	−437.491 078		−25.44	
P6	−437.497 470		−30.52	
TS9	−437.484 359		−24.01	
P7	−437.544 319	−56.13	−65.19	−69.72

[a] Zero point correction has been included in the B3LYP energy differences.

since the migrating group is at nearly 1.9 Å from the receiving C atom, and the N−O' distance value is 2.03−2.10 Å. The optimized B3LYP/6-31G* TS3 obtained geometries are quite similar (Figures 3 and 3S), the larger differences are shown in the H−C'−C'' angle and the H−C'' distance.

The second step going from P2 to P4 is endothermic by 17.31 (R1), 12.37 (R2), and 15.81 (R3) kcal/mol. The transition states connecting the keto and the enol forms, TS4, are at 4.72 (R1), 16.88 (R2), and 8.95 (R3) kcal/mol and show imaginary frequencies of 2164*i* (R1), 2246*i* (R2), and 2184*i* (R3) cm^{-1}, respectively.

For the isobutene case, the corresponding reaction pathway which concerns the anti-Markovnikov oriented adduct, MOp, leading to the formation of carbonyl compounds, P2p, has also been found. The reaction coordinate involves a 1,2-methyl shift

TABLE 3: 2-Methyl-2-butene and NO_3 Radical Reaction. B3LYP/6-31G(d) Total Energies (au), Experimental Enthalpies of Formation, and B3LYP/6-31G(d) and Experimental[38] Energies Relative to the Reactants (kcal/mol) for All PES Stationary Points Relevant to the Theoretical Proposal of the Reaction Mechanism[a]

stationary points	E(B3LYP)	ΔH_f°	ΔE(B3LYP)	ΔH_r°
NO_3 + 2-methyl-2-butene	−476.760 384	7.63	0.00	0.00
TSM	(−476.775 857)		(−7.40)	
TScM	(−476.771 010)		(−4.39)	
MO	−476.793 658		−17.16	
TS1	−476.772 905		−5.85	
P1	−476.825 198		−38.02	
TS3	−476.749 361		6.68	
P2	−476.855 420	−54.86	−57.74	−62.49
TS4	−476.739 060		11.17	
P4	−476.829 717		−42.05	
TS0	−476.768 393		−2.29	
TS5	−476.734 820		16.41	
P5	−476.850 459		−54.13	
MOp	−476.785 134		−12.32	
TS1p	−476.768 069		−2.91	
TS10	−476.771 263		−3.51	
TS11	−476.766 694		−0.79	
M2	−476.814 512		−28.92	
TS8	−476.808 664		−26.44	
P6	−476.811 878		−29.51	
TS9	−476.804 121		−26.04	
P7	−476.873 968	−69.91	−73.19	−77.54

[a] Zero point correction has been included in the B3LYP energy differences. Estimated values are given in parentheses.

from the C' to the C'' carbon atom and the enlargement of the O'−N bond length (see Figure 3). This step is exothermic by 72.13 kcal/mol, and the involved transition state, TS3p, is at 22.69 kcal/mol and shows an imaginary frequency of 495*i* cm^{-1}.

3.4. C−C Cleavage. The third reaction pathway in the global reaction mechanism leads in a first step from MO to an intermediate with a five-member ring structure, M2. The second step gives the nitrite alkoxy radical formation, P6, and then, through a C−C bond cleavage, to the formation of carbonyl compounds, P7, and NO. Three successive transition states, TS10, TS8, and TS9, are involved.

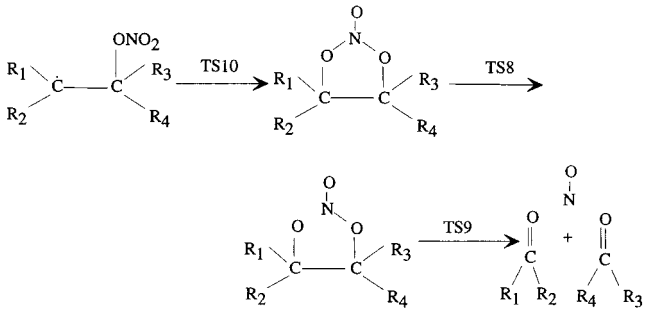

The reaction coordinate leading from MO to M2 involves mainly a dihedral O''−N−O'−C' change. This first step is produced exothermically by 13.49 (R1), 11.00 (R2), 11.76 (R3), and 15.96 (R4) kcal/mol. The involved transition state, TS10, is at −0.61 (R1), −2.09 (R2), −3.59 (R3), and −4.57 (R4) kcal/mol and shows an associated imaginary frequency of 669*i* (R1), 635*i* (R2), 637*i* (R3), and 633*i* (R4) cm^{-1}. For the four mechanisms studied, the geometries of these transition states are quite similar (Figures 4 and 4S).

A pathway leading from the anti-Markovnikov radical adduct, MOp, to M2, through a transition state, TS11, has also been found, for the cases of isobutene and 2-methyl-2-butene. The involved reaction coordinate is similar to that of the corresponding Markovnikov reaction pathway. The transition state, TS11, is at 1.99 (R2) and −0.79 (R3) kcal/mol, showing a corresponding imaginary frequency of 695*i* (R2) and 655*i* (R3) cm^{-1}.

TABLE 4: 2,3-Dimethyl-2-butene and NO_3 Radical Reaction. B3LYP/6-31G(d) Total Energies (au), Experimental Enthalpies of Formation, and B3LYP/6-31G(d) and Experimental[38] Energies Relative to the Reactants (kcal/mol) for All PES Stationary Points Relevant to the Theoretical Proposal of Reaction Mechanism[a]

stationary points	E(B3LYP)	ΔH_f°	ΔE(B3LYP)	ΔH_r°
NO_3 + 2,3-dimethyl-2-butene	−516.073 490	1.32	0.00	0.00
TSM	(−516.089 201)		(−7.47)	
MO	−516.102 311		−14.60	
TS1	−516.086 237		−5.97	
P1	−516.141 176		−40.03	
TS0	−516.086 332		−5.12	
TS10	−516.086 130		−4.57	
M2	−516.130 177		−30.56	
TS8	−516.122 937		−27.16	
P6	−516.124 543		−29.05	
TS9	−516.119 448		−27.15	
P7	−516.199 541	−82.13	−80.87	−83.45

[a] Zero point correction has been included in the B3LYP energy differences. Estimated values are given in parentheses.

The second step in this pathway, going from M2 to P6, is endothermic by 0.59 and 1.51 kcal/mol, for R1 and R4, respectively, and exothermic by 2.69 and 0.59 kcal/mol, for R2 and R3, respectively. The involved transition state, TS8, is at −26.54 (R1), −25.44 (R2), −26.44 (R3), and −27.16 (R4) kcal/mol and shows an imaginary frequency of 175*i* (R1), 195*i* (R2), 164*i* (R3), and 161*i* (R4) cm^{-1}. The reaction coordinate going from M2 to the nitrite alkoxy radical, P6, involves mainly the enlargement of the N−O distance (see Figure 4).

The last step in this pathway leads to formation of the final products, P7, through the homolytic cleavage of the C−C bond, and it is exothermic by 32.74 (R1), 34.67 (R2), 43.68 (R3), and 51.82 (R4) kcal/mol. The reaction coordinate involves the enlargement of the C'−C'' distance and then of the remaining N−O bond to evolve NO, and the shortening of both O'−C' and O''−C'' distances to form the carbonyl groups (see Figure 4). The involved transition state, TS9, is at −24.60 (R1), −24.01 (R2), −26.04 (R3), and −27.15 (R4) kcal/mol and shows an imaginary frequency of 467*i* (R1), 471*i* (R2), 446*i* (R3), and 458*i* (R4) cm^{-1}. Figure 4 shows the B3LYP/6-31G* optimized geometry of the PES stationary points involved in this step. It should be pointed out that the four transition states (see Figure 4) show some small geometrical differences. Thus, the shortest C−C distance corresponds to the 2,3-dimethyl-2-butene case, while the largest one is shown in the isobutene case. Then, the former, showing the largest N−O distance, is a later transition state; i.e., it is more similar to the products than to the reactants.

3.5. Reaction Profiles and E_a. Tables 1−4 show the values of the B3LYP/6-31G* energies of all the stationary points found in the reaction mechanisms of the nitrate radical and, respectively, 2-butene, isobutene, 2-methyl-2-butene, and 2,3-dimethyl-2-butene. Experimental formation and reaction enthalpies[38] of the products and the energies relative to reactants are also shown in Tables 1−4. Schemes of the energy profiles are shown in Figures 5−8. It should be pointed out that the comparison of the experimental energy of stable products (relative to reactants), where available, with B3LYP/6-31G* values gives differences in the range of 1−5 kcal mol^{-1}, except for P7 in the NO_3 + 2-butene reaction, where the difference is 11.17 kcal mol^{-1}.

In all the cases studied in this work, an initial transition state of energy lower than reactants leads from the reactants to either the Markovnikov or anti-Markovnikov radical adducts. A

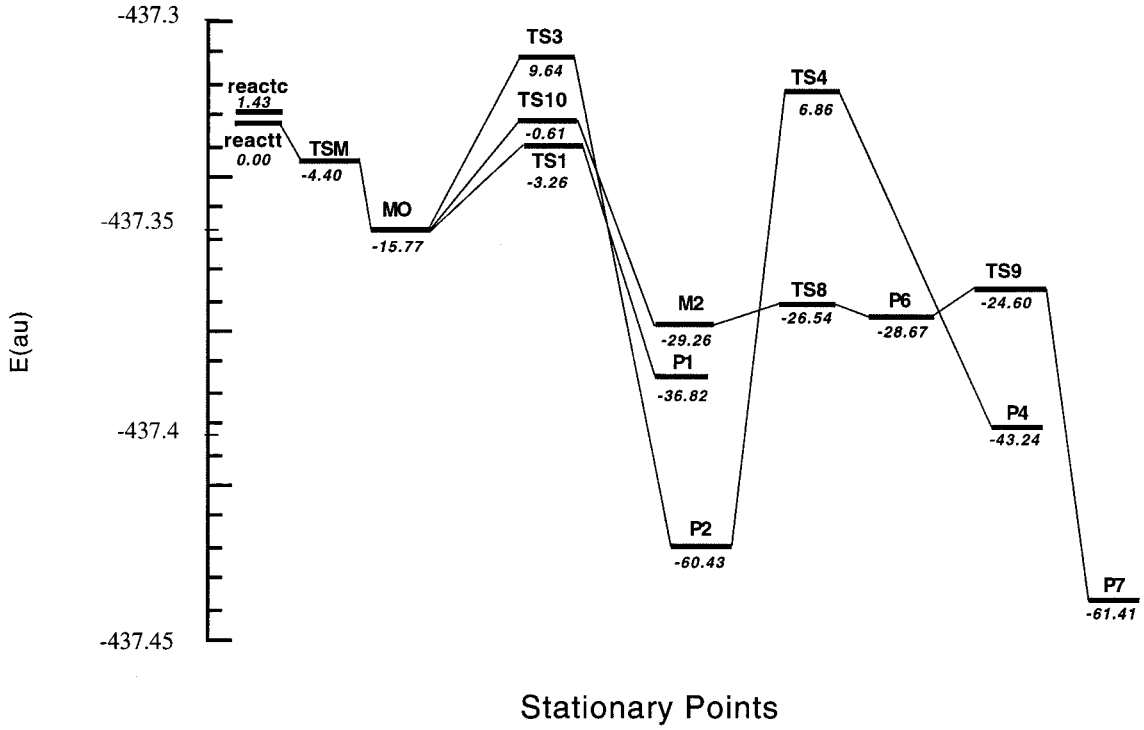

Figure 5. Addition reaction 2-butene + NO_3: Scheme of the reaction profile at the B3LYP/6-31G* level of theory. The energy values (kcal/mol) are relative to reactants.

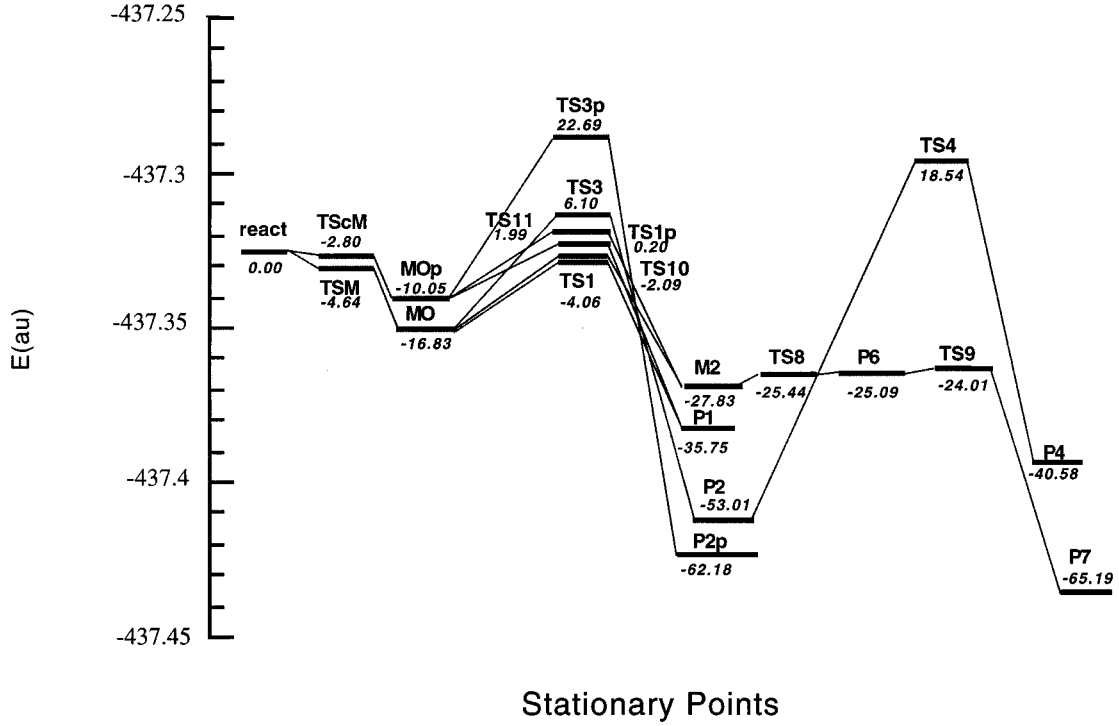

Figure 6. Addition reaction isobutene + NO_3: Scheme of the reaction profile at the B3LYP/6-31G* level of theory. The energy values (kcal/mol) are relative to reactants.

transition state with less energy than the reactants has physical sense if a previous van der Waals complex is formed between the reactants, as in the case of the NO_3 + ethene reaction mechanism.[23] The van der Waals complexes have not been searched, since they are very difficult to find at the DFT level, and, moreover, they are not chemically relevant in the reaction mechanisms,[39] although they will probably exist.

Since the experimental E_a is measured from the disappearance rate of the NO_3 radical, its value must be related with the relative to reactants energy of the initial transition state leading to the radical adduct. We have only found in the literature the value of the experimental E_a for the case of 2-butene,[1] which is 0.6 kcal/mol. The energy relative to reactants for the initial transition state for this reaction, as obtained theoretically, is −4.4 kcal/mol. The uncertainty of the experimental activation energy values is about 30%, and the theoretical values of the energy barriers at B3LYP/6-31G* level are affected by an uncertainty of nearly 0.5 eV. Then, both theoretical and experimental values

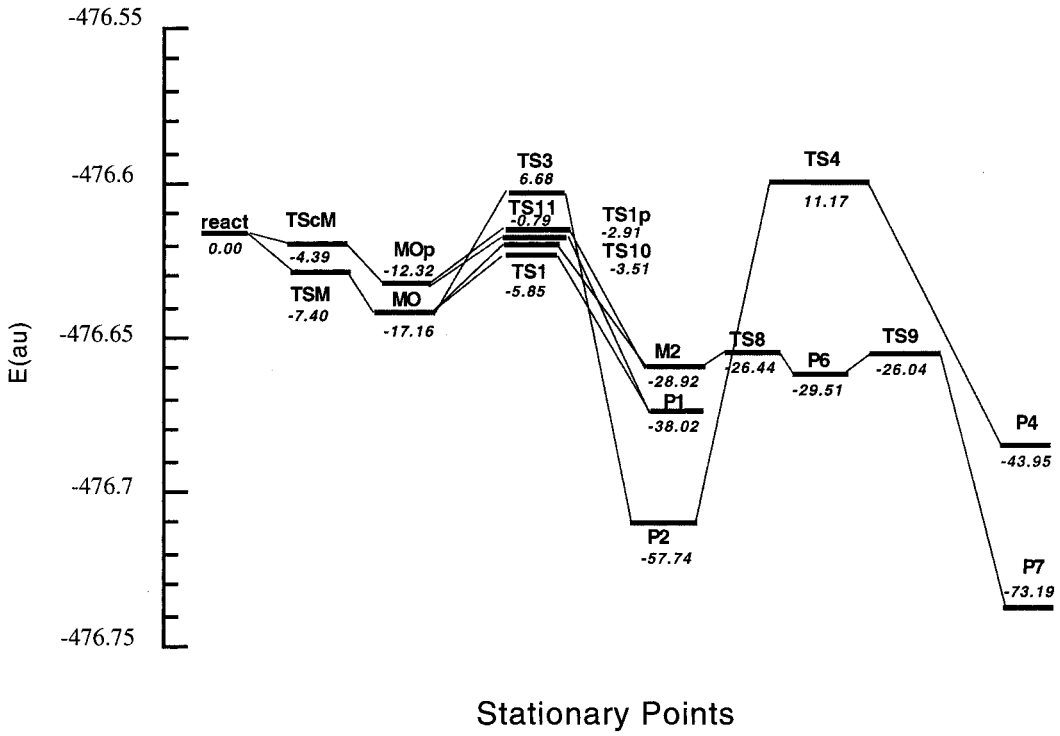

Figure 7. Addition reaction 2-methyl-2-butene + NO_3: Scheme of the reaction profile at the B3LYP/6-31G* level of theory. The energy values (kcal/mol) are relative to reactants.

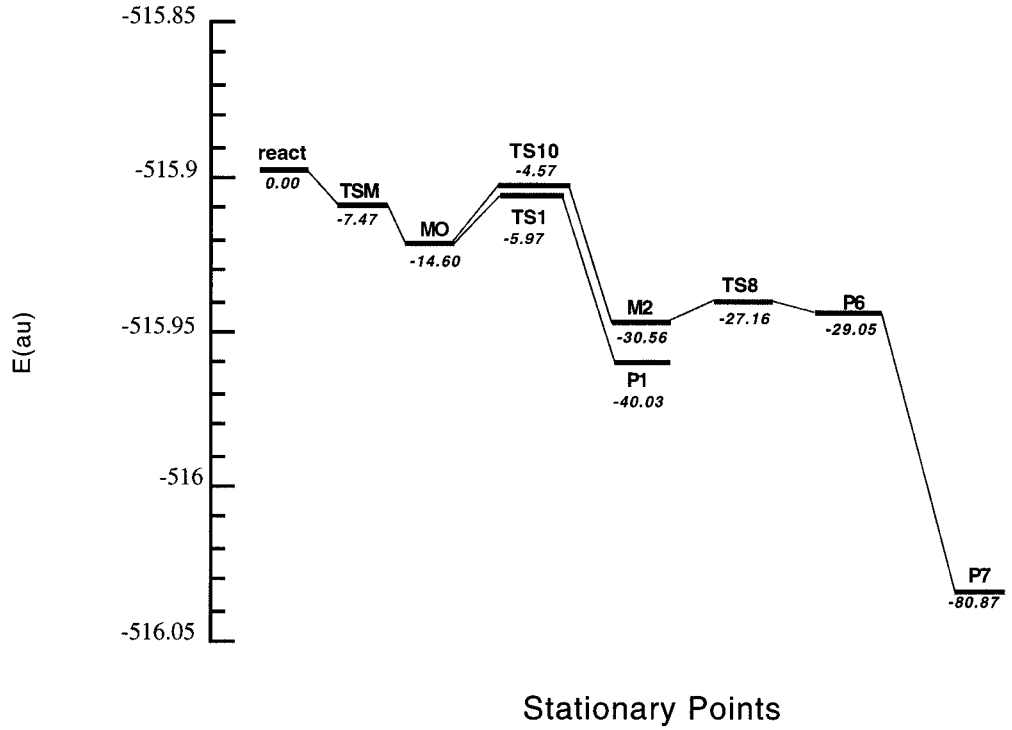

Figure 8. Addition reaction 2,3-dimethyl-2-butene + NO_3: Scheme of the reaction profile at the B3LYP/6-31G* level of theory. The energy values (kcal/mol) are relative to reactants.

are in the confidence range for each other. In any case, B3LYP/6-31G* tends to give transition states too low in energy (lower energy barriers) than other more accurate methods.[26]

The reactants will enter in the reaction channel at energy higher than the initial transition state or after overcoming a small barrier, depending on whether the initial transition state has lower energy than reactants or slightly higher. As it can be seen in Figures 5−8, the transition states that lead to either the epoxide + NO_2 formation or the C−C cleavage products are also lower in energy than the reactants. Then, we can expect that all the intermediates and products in these two pathways will be directly accessible in the reaction channel. However, the branching between the possible channels is linked by the rates of passing over the corresponding transition states. Then, even if MO (MOp) has energy enough to overcome both TS1 (TS1p) and TS10 (TS11) transition states, we can expect that P1 will show the greatest final concentration, as it is experimentally found at low pressures under inert gas conditions. This

conclusion involves that the entropies of both transition states are similar and that the reverse reaction rates can be neglected. In aerobic conditions, oxygen would attack the radical adduct to give peroxides.[8]

In all the reaction mechanisms shown in this work, the reaction step pathway leading from MO or MOp to either aldehydes or ketones by means of a 1,2- hydrogen shift involves energy barriers of 6−9 kcal mol^{-1}. Therefore, these steps can be discarded in tropospheric conditions, but for higher temperatures.

The whole resulting mechanisms are the same for the four studied reactions, so the effect on the reaction mechanism of the number and position of the methyl substituents on the double bond is not very great. Along with the results of previous works[9,10,23] we can conclude that the greater the number of substituents on the double bond, the more negative are the energies relative to reactants of the initial transition states, and, then, the rate coefficients will be greater, in agreement with experimental data.[40] Also, when the number of methyl groups on the double bond increases, the energy relative to reactants of the transition states leading to the C−C cleavage products becomes more negative, this pathway being more favorable from a kinetic point of view. This fact is also in agreement with experimental data, since it is known that the quantity of carbonyl compounds increases as the number of methyl groups on the double bond increases.[3,41]

4. Conclusions

The theoretical study of the addition reaction of the NO_3 radical to 2-butene, isobutene, 2-methyl-2-butene, and 2,3-dimethyl-2-butene has been carried out. This study includes geometry optimization and characterization of the stationary points at density functional theory using the B3LYP/6-31G* functional and basis set. The initial transition state, leading from the reactants to the initial adduct, is obtained lower in energy than the reactants, showing that this step is kinetically favored. For the isobutene and 2-methyl-2-butene, where the two carbon atoms at both sides of the double bond are not symmetrically substituted, the addition reactions giving the Markovnikov- and anti-Markovnikov-oriented adducts have been obtained. In the proposed general reaction mechanism, three main reaction pathways have been found. The first reaction pathway leads to the formation of epoxide and NO_2, products that are those proposed experimentally.[5] The second pathway leads to the formation of carbonyl compounds, and the third one leads, through the cleavage of the C−C bond, to carbonyl compounds with a lower number of carbon atoms than the reactant. According to the theoretically proposed mechanisms, the different obtained products would be as follows: (a) for the R1 reaction, 2,3-dimethyloxirane, butanone, and ethanal; (b) for the R2 reaction, 2-methylepoxypropane, 2-methylpropanal, butanone, propanone, and formaldehyde; (c) for the R3 reaction, 2-methylepoxybutane, 3-methylbutanone, propanone, 2-dimethylpropanal, and ethanal; (d) for the R4 reaction, 2,3-dimethylepoxybutane, 3-dimethylbutanone, and propanone. In any case, NO_2 and NO are also obtained as products.

From the mechanism proposed in this work, we can conclude that, at low temperatures and low pressures in anaerobic conditions, in agreement with the experimental data,[5,8] the epoxide and NO_2 will be the main products. The products resulting from the C−C cleavage (aldehydes, ketones, and NO) will have increasing importance as the substitution degree increases.

At higher temperatures, as in the combustion processes, the system could have enough energy to overcome the barrier leading to the formation of carbonyl compounds through a 1,2-hydrogen shift, but this pathway will not be very likely in the troposphere.

Acknowledgment. M.P.P. thanks the Ministerio de Educación y Ciencia for a personal grant. This work was supported by Spanish DGICYCT (Project PB97-1381), and CCEC (Project INF99-02-134).

Supporting Information Available: Figures 1S−4S including the optimized geometries of the PES stationary points for the reaction mechanism of the NO_3 addition to 2-methyl-2-butene (R3) and 2,3-dimethyl-2-butene (R4). This material is available free of charge via the Internet at http://acs.pubs.org.

References and Notes

(1) Wayne, R. P.; Barnes, I.; Biggs, P.; Burrows, J. P.; Canosa-Mas, C. E.; Hjorth, J.; Bras, G. L.; Moortgat, G. K.; Perner, D.; Poulet, G.; Restelli, G.; Sidebottom, H. *Atmos. Environ.* **1991**, *25A*, 1.

(2) Atkinson, R. *J. Phys. Chem. Ref. Data* **1991**, *20*, 459.

(3) Hjorth, J.; Lohse, C.; Nielsen, C. J.; Skov, H.; Restelli, G. *J. Phys. Chem.* **1990**, *94*, 7494.

(4) Wille, U.; Rahman, M. M.; Schindler, R. N. *Ber. Bunsen-Ges. Phys. Chem.* **1992**, *96*, 833.

(5) Wille, U.; Schindler, R. N. *Ber. Bunsen-Ges. Phys. Chem.* **1993**, *97*, 1447.

(6) Skov, H.; Benter, T.; Schindler, R. N.; Hjorth, J.; Restelli, G. *Atmos. Environ.* **1994**, *28*, 1583.

(7) Berndt, T.; Böge, O. *Ber. Bunsen-Ges. Phys. Chem.* **1994**, *98*, 869.

(8) Berndt, T.; Böge, O. *J. Atmos. Chem.* **1995**, *21*, 275.

(9) Pérez-Casany, M. P.; Nebot-Gil, I.; Sánchez-Marín, J.; Tomás-Vert, F.; Martínez-Ataz, E.; Cabañas-Galán, B.; Aranda-Rubio, A. *J. Org. Chem.* **1998**, *63*, 6978.

(10) Pérez-Casany, M. P.; Nebot-Gil, I.; Sánchez-Marín, J. *J. Phys. Chem.* **2000**, *104*, 6277.

(11) Dewar, M. J. S.; Zoebisch, E. G.; Healy, E. F.; Stewart, J. J. P. *J. Am. Chem. Soc.* **1985**, *107*, 3902.

(12) Pérez-Casany, M. P.; Nebot-Gil, I.; Sánchez-Marín, J. *J. Am. Chem. Soc.*, in press.

(13) Slater, J. C. *Quantum Theory of Molecular and Solids*; McGraw-Hill: New York, 1974; Vol. 4.

(14) Fock, V. *Z. Physic* **1930**, *61*, 126.

(15) Becke, A. D. *Phys. Rev. A* **1988**, *38*, 3098.

(16) Vosko, S. H.; Wilk, L.; Nusair, M. *J. Chem. Phys.* **1987**, *87*, 5968.

(17) Lee, C.; Yang, W.; Parr, R. G. *Phys. Rev. B* **1988**, *37*, 385.

(18) Baker, J. *J. Comput. Chem.* **1986**, *7*, 385.

(19) Schlegel, H. B. *J. Comput. Chem.* **1982**, *3*, 214.

(20) Hehre, W.; Radom, L.; Schleyer, P.; Pople, J. *Ab Initio Molecular Orbital Theor.*; Wiley-Interscience: New York, 1986.

(21) Hariharan, P.; Pople, J. *Chem. Phys. Lett.* **1972**, *16*, 217.

(22) Frisch, M. J.; Trucks, G. W.; Schlegel, H. B.; Gill, P. M. W.; Johnson, B. G.; Robb, M. A.; Cheeseman, J. R.; Keith, T.; Petersson, G. A.; Montgomery, J. A.; Raghavachari, K.; Al-Laham, M. A.; Zakrzewski, V. G.; Ortiz, J. V.; Foresman, J. B.; Cioslowski, J.; Stefanov, B. B.; Nanayakkara, A.; Challacombe, M.; Peng, C. Y.; Ayala, P. Y.; Chen, W.; Wong, M. W.; Andres, J. L.; Replogle, E. S.; Gomperts, R.; Martin, R. L.; Fox, D. J.; Binkley, J. S.; Defrees, D. J.; Baker, J.; Stewart, J. P.; Head-Gordon, M.; González, C.; Pople, J. A. *GAUSSIAN 94*, Revision D.3; Gaussian Inc.: Pittsburgh, PA, 1995.

(23) Pérez-Casany, M. P.; Nebot-Gil, I.; Sánchez-Marín, J.; Crespo-Crespo, R. To be published.

(24) Singleton, D. L.; Cvetovic, R. J., *J. Am. Chem. Soc.* **1976**, *98*, 6812.

(25) Mozurkewich, M.; Benson, S. W., *J. Phys. Chem.* **1984**, *88*, 6429. Mozurkewich, M.; Lamb, J. J.; Benson, S. W. *J. Phys. Chem.* **1984**, *88*, 6435.

(26) Piqueras, M. C.; Crespo, R.; Nebot-Gil, I.; Tomás, F. Submitted for publication.

(27) Alvarez-Idaboy, J. R.; Díaz-Acosta, I.; Vivier-Bunge, A. *J. Comput. Chem.* **1998**, *88*, 811.

(28) Díaz-Acosta, I.; Alvarez-Idaboy, J. R.; Vivier-Bunge, A. *Int. J. Chem. Kinet.* **1999**, *31*, 29.

(29) Alvarez-Idaboy, J. R.; Mora-Díez, N.; Vivier-Bunge, A. *J. Am. Chem. Soc.* **2000**, *122*, 3715.

(30) Greiner, N. R. *J. Chem. Phys.* **1970**, *53*, 1284.

(31) Tully, F. P. *Chem. Phys. Lett.* **1983**, *96*, 148.

(32) Atkinson, R.; Perry, R. A.; Pitts, J. N., Jr. *J. Chem. Phys.* **1977**, *66*, 1197.

(33) Zellner, R.; Lorenz, K. *J. Phys. Chem.* **1984**, *88*, 984.

(34) Diau, E. W. G.; Lee, Y.-P. *J. Chem. Phys.* **1992**, *96*, 377.
(35) Sosa, C.; Schlegel, H. B. *J. Am. Chem. Soc.* **1987**, *109*, 4193.
(36) Villà, J.; González-Lafont, M. A.; Lluch, J. M.; Corchado, J. C.; Espinosa-García, J. *J. Chem. Phys.* **1997**, *107*, 7266.
(37) Sekusak, S.; Liedl, K. R.; Sablic, A. *J. Phys. Chem.* **1998**, *102*, 1583.
(38) Lide, D. R. *Handbook of Chemistry and Physics*; CRC Press: Boca Raton, FL, 1996.
(39) García-Cruz, I.; Ruiz-Santoyo, M. E.; Alvarez-Idaboy, J. R.; Vivier-Bunge, A. *J. Comput. Chem.* **1999**, *20*, 845.
(40) Atkinson, R.; Baulch, D. L.; Cox, R. A.; R. F. Hampson, J.; Kerr, J. A.; Rossi, M. J.; Troe, J. *J. Phys. Chem. Ref. Data* **1997**, *26*, 1329.
(41) Barnes, I.; Bastian, V.; Becker, K. H.; Tong, Z. *J. Phys. Chem.* **1990**, *94*, 2413.